Acta Pharmaceutica Sinica B 2021;11(12):4045–4054

Chinese Pharmaceutical Association
Institute of Materia Medica, Chinese Academy of Medical Sciences

Acta Pharmaceutica Sinica B

www.elsevier.com/locate/apsb
www.sciencedirect.com

SHORT COMMUNICATION

Baicalin induces ferroptosis in bladder cancer cells by downregulating FTH1

Na Kong[a,c,†], Xiaying Chen[a,b,†], Jiao Feng[a,b], Ting Duan[a,b], Shuiping Liu[a,b], Xueni Sun[a,b], Peng Chen[a,b], Ting Pan[a,b], Lili Yan[a,b], Ting Jin[a,b], Yu Xiang[a,b], Quan Gao[a,b], Chengyong Wen[a,b], Weirui Ma[a,b], Wencheng Liu[a,b], Mingming Zhang[a,b], Zuyi Yang[a,b], Wengang Wang[a,b], Ruonan Zhang[a,b], Bi Chen[a,b], Tian Xie[a,b,*], Xinbing Sui[a,b,*], Wei Tao[c,*]

[a]*College of Pharmacy and Department of Medical Oncology, the Affiliated Hospital of Hangzhou Normal University, School of Medicine, Hangzhou Normal University, Hangzhou 311121, China*
[b]*Key Laboratory of Elemene Class Anti-Cancer Chinese Medicines; Engineering Laboratory of Development and Application of Traditional Chinese Medicines; Collaborative Innovation Center of Traditional Chinese Medicines of Zhejiang Province, Hangzhou Normal University, Hangzhou 311121, China*
[c]*Center for Nanomedicine and Department of Anesthesiology, Brigham and Women's Hospital, Harvard Medical School, Boston, MA 02115, USA*

Received 1 February 2021; received in revised form 7 March 2021; accepted 11 March 2021

KEY WORDS

Baicalin;
Ferroptosis;
Bladder cancer;
FTH1;
Deferoxamine

Abstract Ferroptosis is a non-apoptotic regulated cell death caused by iron accumulation and subsequent lipid peroxidation. Currently, the therapeutic role of ferroptosis on cancer is gaining increasing interest. Baicalin an active component in *Scutellaria baicalensis* Georgi with anticancer potential various cancer types; however, the effects of baicalein on bladder cancer and the underlying molecular mechanisms remain largely unknown. In the study, we investigated the effect of baicalin on bladder cancer cells 5637 and KU-19-19. As a result, we show baicalin exerted its anticancer activity by inducing apoptosis and cell death in bladder cancer cells. Subsequently, we for the first time demonstrate baicalin-induced ferroptotic cell death *in vitro* and *in vivo*, accompanied by reactive oxygen species (ROS) accumulation and intracellular chelate iron enrichment. The ferroptosis inhibitor deferoxamine but not necrostatin-1, chloroquine (CQ), *N*-acetyl-L-cysteine, L-glutathione reduced, or carbobenzoxy-valyl-alanyl-aspartyl-[*O*-methyl]-fluoromethylketone (Z-VAD-FMK) rescued baicalin-induced cell death, indicating

*Corresponding authors.
E-mail addresses: xbs@hznu.edu.cn (Tian Xie), hzzju@hznu.edu.cn (Xinbing Sui), wtao@bwh.harvard.edu (Wei Tao).
†These authors made equal contributions to this work.
Peer review under responsibility of Chinese Pharmaceutical Association and Institute of Materia Medica, Chinese Academy of Medical Sciences.

https://doi.org/10.1016/j.apsb.2021.03.036

ferroptosis contributed to baicalin-induced cell death. Mechanistically, we show that ferritin heavy chain 1 (FTH1) was a key determinant for baicalin-induced ferroptosis. Overexpression of FTH1 abrogated the anticancer effects of baicalin in both 5637 and KU19-19 cells. Taken together, our data for the first time suggest that the natural product baicalin exerts its anticancer activity by inducing FTH1-dependent ferroptosis, which will hopefully provide a prospective compound for bladder cancer treatment.

1. Introduction

Ferroptosis is a recently discovered non-apoptotic modality of regulatory cell death, which is driven by iron-dependent, lipid peroxidation, membrane damage, and cell lysis[1−3]. Previous studies have demonstrated that ferroptosis is involved in the onset and development of numerous diseases, including ischemia−reperfusion injury, cardiovascular diseases, acute kidney injury, and neurodegenerative disorders[4,5]. Recently, increasing studies have confirmed that ferroptosis contributes to eliminating cancer cells in an apoptosis-independent manner[6,7]. Therefore, ferroptosis is attracting more and more attention due to its effectiveness in cancer treatment.

Scutellaria baicalensis Georgi or Huangqin, as a medicinal plant, is used widely in many Asian countries especially in China. Baicalin, a monomer of Chinese traditional herbs extracted from *S. baicalensis* Georgi, exhibits its antitumor effects on several tumor progression. Baicalein in combination with baicalin enhanced the growth-inhibition effect of human breast cancer cells through the ERK/p38 MAPK pathway[8]. Baicalin initiated reprogramming of tumor-associated macrophages into M1-like macrophages and promoted the production of pro-inflammatory cytokines. Co-treatment with tumor-associated macrophages and baicalin led to a decrease in its motility and proliferation of hepatocellular carcinoma[9]. Baicalin nanoliposomes showed a better antitumor therapeutic efficacy for lung cancer compared with their controls[10]. Baicalin treatment triggered autophagic cell death in T24 cells by blocking AKT/protein kinase B signaling pathway[11]. However, the function of baicalin in bladder cancer remains largely unknown.

In the study, we investigated the effect of baicalin on bladder cancer cells 5637 and KU-19-19. As a result, we found that baicalin exhibited its anticancer activity by inducing apoptosis and cell death in bladder cancer cells in a dose-dependent manner. Subsequently, we for the first time demonstrated baicalin-induced ferroptotic cell death *in vitro* and *in vivo*, accompanied by reactive oxygen species (ROS) accumulation and intracellular chelate iron enrichment. Subsequently, we showed that ferritin heavy chain 1 (FTH1) was a key determinant for baicalin-induced ferroptosis. Overexpression of FTH1 abrogated the anticancer effects of baicalin in bladder cancer cells. Taken together, our data for the first time suggest that baicalin exerts its anticancer function by triggering FTH1-dependent ferroptosis, which may provide a potential anticancer drug for bladder cancer treatment.

2. Materials and methods

2.1. Cell culture

The 5637 and KU-19-19 cell lines were obtained from ATCC, and maintained in RPMI-1640 medium with 10% fetal bovine serum, 100 units/mL penicillin, and 100 μg/mL streptomycin comprising 5% CO_2 controlling the temperature at 37 °C.

2.2. Reagents and antibodies

All primary antibody subsequent experiments used were anti-BAX antibody (Cell Signaling, 14796S), anti-53BP1 antibody (Cell Signaling, 4937), anti-α-tubulin antibody (Sigma, T8203), anti-transferrin antibody (Abcam, ab82411), anti-FTH1 antibody (Cell Signaling, 4393S), anti-heme oxygenase-1 antibody (HO-1, Abcam, ab189491), anti-ferritin antibody (Abcam, ab75937), anti-cleaved caspase-3 antibody (Abcam, ab2302), anti-β-actin antibody (Cell Signaling, 12262S), anti-γ-H2AX antibody (Millipore, 2652964), anti-P53 antibody (Novus, NB200-103). And reagents mentioned in experiments were purified baicalin (>98%, Shanghai Yuanye, B20570), deferoxamine mesylate (DFO, Selleck, S5742), Z-VAD-FMK (MCE, HY-16658B), chloroquine (CQ, Sigma, C6628), necrostatin-1 (Nec-1, MCE, HY-15760), *N*-acetylcysteine (NAC, MCE, HY-B0215), L-glutathione reduced (GSH, MCE, HY-D0187), FTH1 tagged ORF clone (Origene, RC209845).

2.3. Cell viability assay

The cell viability of 5637 and KU-19-19 with the baicalin treatments was determined using CCK8 (Meilunbio, Cat.: MA0218). About 4.5×10^3 cells per well were seeded into 96-well plates. And then treated with various concentrations of baicalin with or without inhibitor or inducer for 24 h. After treatment, 100 μL per well RPMI-1640 medium including 10 percentage CCK-8 was added in wells and incubated at 37 °C for 1−4 h and then measured at 450 nm wavelength[12].

2.4. Colony-formation assay

About 3×10^3 cells per well were seeded in 100 mm plates. The cells were maintained for about 18 days until the cells grew to visible colonies. Then KU-19-19 or 5637 were maintained in RPMI-1640 medium with two concentrates of baicalin for 1 day and change into normal RPMI-1640 medium for two days. The same operation needs to repeat about 3 times. Then colonies in every plate were fixed by 4% paraformaldehyde and stained by crystal violet solution for 1 h at room temperature.

2.5. Real-time quantitative PCR (qRT-PCR)

About 2×10^5 cells were added in 60 mm dishes and given different treatments. RNA was extracted (Trizol, Ambion) and reversed (Vazyme Biotech, Cat.: R323-01) to cDNA. RNA extracted from the treated cells was prepared for RNA-seq

experiments, as described previously[13]. qPCR reactions were performed (Vazyme, Biotech, Cat.: Q711) and the program of qPCR was followed by instruction. The primers for GAPDH were a forward primer, 5′-GTC TCC TCT GAC TTC AAC AGC G-3′, and a reverse primer, 5′-ACC ACC CTG TTG CTG TAG CCA A-3′. The primers for TF were a forward primer, 5′-TCA GCA GAG ACC ACC GAA GAC T-3′, and a reverse primer, 5′-GAC CAC ACT TGC CCG CTA TGT A-3′.

2.6. *Mitochondria mass assessment*

Mito-Tracker Green was used to measure the mitochondria mass of 5637 and KU-19-19 cells. And fluorescence intensity and quantity reflect the number and mass of mitochondria. Mitochondria was a multifaceted regulator of cell death including necroptosis, ferroptosis, pyroptosis, and programmed cell death[14–16]. The cells were added in 60 mm plates and given different treatments. After 24 h, cells were dyed with 20 nmol/L Mito-Tracker Green (Beyotime Biotechnology, Cat.: C1048) for 1 h and 1 μg/mL Hoechst 33342 (Beyotime Biotechnology, Cat.: C1022) for 10 min. The results were analyzed by a positive fluorescence microscope.

2.7. *Measurement of intracellular chelate iron*

About 4×10^5 cells were added in 60 mm plates. 5637 and KU-19-19 were treated as indicated for 24 h after attachment. Living cells were collected and stained by Phen Green SK (ThermoFisher, Cat.: P14313) according to the manufacturer's instructions. The fluorescent degree was analyzed by a flow cytometer (Beckman Coulter, CytoFLEX S).

2.8. *Measurement of ROS*

About 3×10^5 cells were added in 60 mm plates. After attachment overnight, cells were treated differently for 24 h, and then replaced with serum-free medium containing 10 μmol/L DCFH-DA, (Beyotime Biotechnology, Cat.: S0033) for 0.5−1 h. Cells were washed twice with PBS to get rid of remnant DCFH-DA. Then, the cells were resuspended in 300 μL PBS, and the ROS generation was analyzed by flow cytometer with about 10,000 labeled cells analyzed[17].

2.9. *Apoptosis assays*

The percent of apoptosis in cells was assayed according to the instructions (BD, 556547). About 2×10^5 cells were added in 60 mm dishes and given different treatments. After treatments for 24 h, the cells were collected and resuspended in 300 μL ice-cold 1 × binding buffer and dyed with PI and FITC Annexin V about 30 min at 4 °C in the dark. The results were analyzed by a flow cytometer.

2.10. *Western blotting analysis*

About 8×10^5 cells were added in 100 mm dishes. After attachment, the cells were given different treatments for 24 h. Then collected cells had been lysed in RIPA (Beyotime Biotechnology, Cat.: P0013B) for 30 min on ice. After centrifuged at 10,000 rpm (Eppendorf AG, type: 5430R, Barhausenweg 1 22339 Hamburg, Germany), the supernatant was collected and quantified the protein concentrations by the BCA Protein Assay Kit (Beyotime Biotechnology, Cat.: P0010). Equal amounts (15 μg) of total protein were resolved in 12% SDS-PAGE and then transferred to PVDF membranes (Millipore, Cat.: ISEQ00010). Membranes with proteins were conducted to blocking, washing, incubation with antibodies, and finally detection with enhanced chemiluminescence.

2.11. *In vivo bladder tumor model*

All mouse experiments were approved by the Use and Care of Animals Committee at Hangzhou Normal University. About 6×10^6 KU-19-19 cells were injected into the about 3−5 weeks old female BALB/c nude mice (about 18 g, $n = 5$). Tumor dimensions were measured every 2 days by digital caliper, and the tumor volume (V) was calculated by Eq. (1):

$$V = (\text{Maximal length} \times \text{Maximal width}^2)/2 \quad (1)$$

Once palpable tumors appeared, the mice were randomized in four groups: the control (deionized water containing 7% Tween 80 and 0.1% CMC-Na) group, the DFO (100 mg/kg/day) group, the baicalin (200 mg/kg/day) group, and DFO + baicalin group. After 10 days of drug administration (intraperitoneal injection, once daily), mice were sacrificed, and tumor specimens resected were collected for immunohistochemical staining and Perl's staining (Solarbio Life Sciences, G1420).

2.12. *Statistical analysis*

Unless otherwise stated, three times at least in all studies were performed. The results are expressed with mean ± standard deviation (SD). The significance of the results in statistics was determined by the t-test in Graphpad Prism.

3. Results

3.1. *Baicalin triggered cell death and inhibited cell proliferation in bladder cancer cells*

To investigate the effect of baicalin, two human bladder cancer cell lines 5637 and KU-19-19 were treated with different concentrations of baicalin for 24 h. As a result, the cell counting Kit-8 (CCK-8) assay showed baicalin-induced cell death of bladder cancer in a dose-dependent manner (Fig. 1A). Cell apoptosis was assessed by annexin V-FITC/PI staining. The results show that a high percentage of cell death and apoptosis was found in 5637 and KU-19-19 cells after the treatment with baicalin (Fig. 1B and C). To examined the effect of baicalin on cell proliferation, the colony formation assay was made. As a result, baicalin treatment significantly inhibited colony formation (Fig. 1D and E). These results indicate that baicalin treatment triggered cell death and inhibited cell proliferation of bladder cancer cells.

In the next study, we analyzed the expression of several apoptotic and ferroptotic proteins in bladder cancer cells after the baicalin treatment by Western blotting. The data suggest baicalin treatment promoted apoptosis in bladder cancer cells (Fig. 1F). As we know, ferroptosis was also involved in cancer cell death. So, we detected the expression of several iron regulatory proteins. Western blotting showed that increased transferrin, phosphorylated histone H2AX (γ-H2AX), P53, tumor suppressor P53 binding protein 1 (53BP1) and decreased FTH1 were found in baicalin-treated bladder cancer cells. These data suggest baicalin

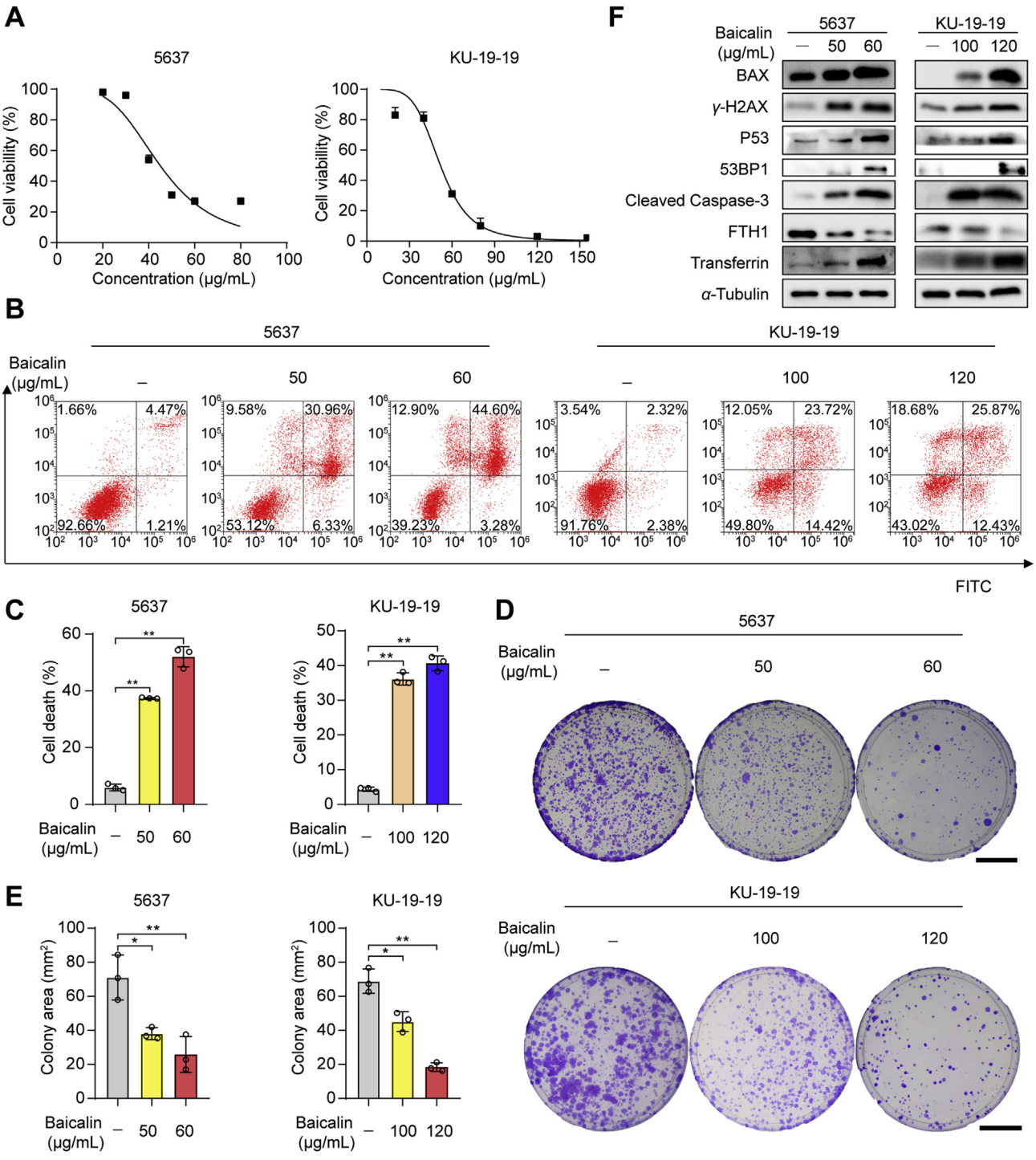

Figure 1 The cell viability of 5637 and KU-19-19 cells was detected after the treatment with baicalin. (A) The cell viability of 5637 and KU-19-19 was examined by CCK-8 assay after the treatment with various concentrations of baicalin for 24 h. (B) and (C) Representative results of annexin V-FITC/PI staining and quantitative analysis after the treatment with baicalin for 24 h, mean ± SD, $n = 3$; $^{*}P < 0.05$, $^{**}P < 0.01$. (D) and (E) Representative results of the colony formation and quantitative analysis, mean ± SD, $n = 3$; $^{*}P < 0.05$, $^{**}P < 0.01$. Scale: 30 mm. (F) The expression of BCl-2-associated X (BAX), P53 binding protein 1 (53BP1), phosphorylated histone H2AX (γ-H2AX), P53, ferritin heavy chain 1 (FTH1), transferrin, and cleaved caspase-3 was determined by Western blotting.

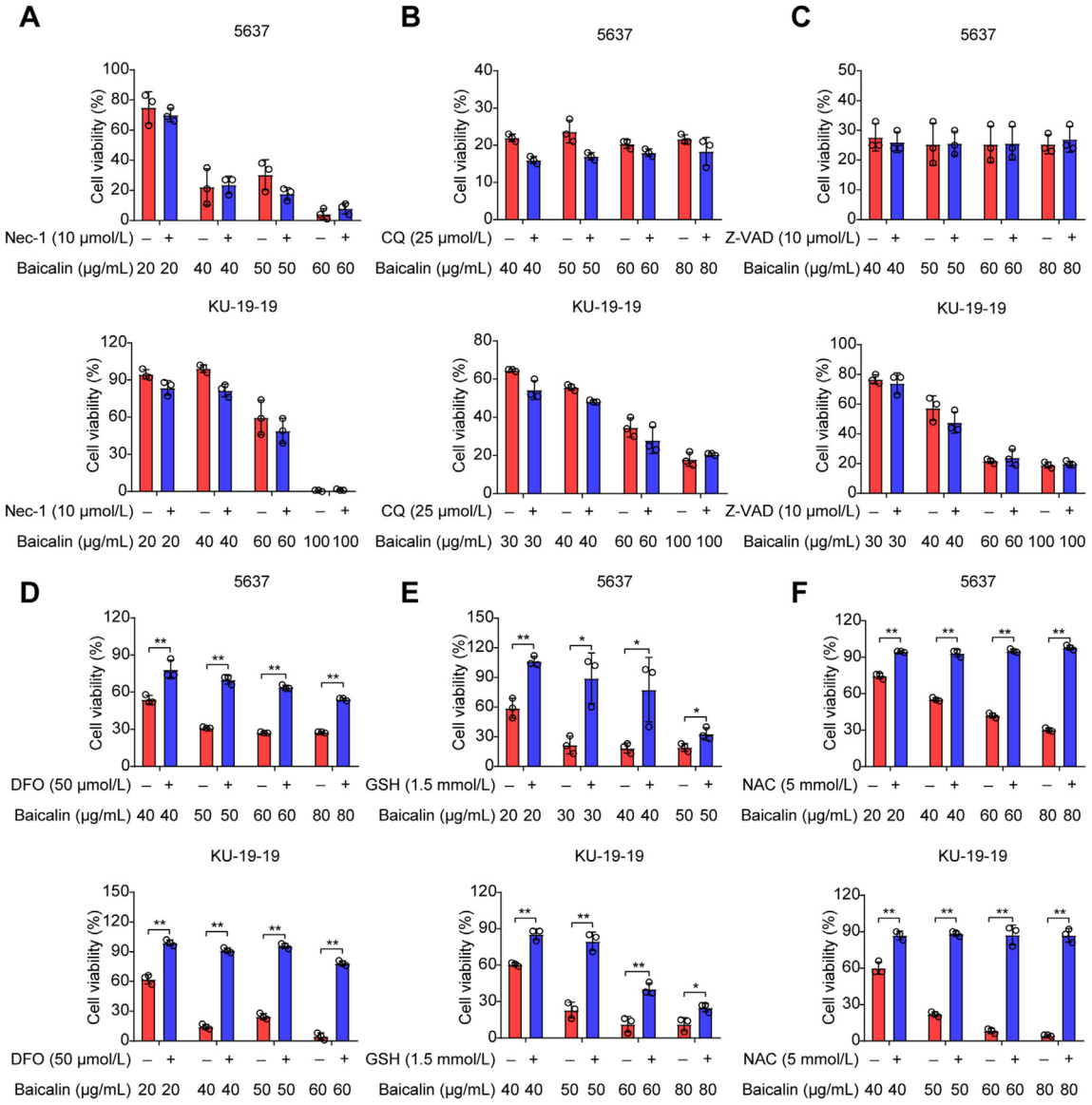

Figure 2 The effect of baicalin alone or in combination with other cell death inhibitors on the inhibition of growth of bladder cancer cells. (A) 5637 and KU-19-19 were treated with baicalin accompanied with or without Nec-1 for 24 h, then cell viability was tested. (B) 5637 and KU-19-19 were treated with baicalin along with or without chloroquine (CQ) for 24 h, then cell viability was tested. (C) Pretreatment with or without carbobenzoxy-valyl-alanyl-aspartyl-[*O*-methyl]-fluoromethylketone (Z-VAD-FMK), 5637 and KU-19-19 cells were treated with baicalin for 24 h, then cell viability was assayed. (D) 5637 and KU-19-19 were treated with baicalin with or without deferoxamine (DFO) for 24 h and cell viability was analyzed, $^{**}P < 0.01$. (E) 5637 and KU-19-19 were treated with baicalin with or without glutathione (GSH) for 24 h, then cell viability was analyzed, mean ± SD, $n = 3$; $^{*}P < 0.05$, $^{**}P < 0.01$. (F) 5637 and KU-19-19 were treated with baicalin along with or without *N*-acetylcysteine (NAC) for 24 h and the cell viability was assayed, mean ± SD, $n = 3$; $^{**}P < 0.01$.

treatment could induce apoptosis, oxidative DNA damage[18] and ferroptosis in bladder cancer.

3.2. *Ferroptosis contributed to baicalin-induced cell death in bladder cancer cells*

To determine which cell death form dominantly contributed to the cell death induced by baicalin, several inhibitors of different cell death pathways were utilized. The co-treatment with chloroquine (CQ, autophagy inhibitor), necrostatin-1 (Nec-1, necroptosis inhibitor), or Z-VAD-FMK (pan-caspase inhibitor) could not significantly reverse baicalin-caused cell death in bladder cancer cells (Fig. 2A–C). Whereas, the ferroptosis inhibitor deferoxamine (DFO), oxygen-derived free radicals scavenger glutathione (GSH) and ROS inhibitor *N*-acetylcysteine (NAC) remarkably rescued baicalin-induced cell death (Fig. 2D–F). Moreover, baicalin-induced cell death was almost rescued through co-treatment with iron chelator DFO (Fig. 3A and B). These results indicate ferroptosis as the predominant method that contributed to baicalin-induced cell death.

It is known that intracellular iron and ROS accumulation are critical events in ferroptosis. Thus, intracellular chelate iron was determined by using the fluorescent indicator Phen Green SK, the fluorescence of which is quenched by iron. As expected, baicalin

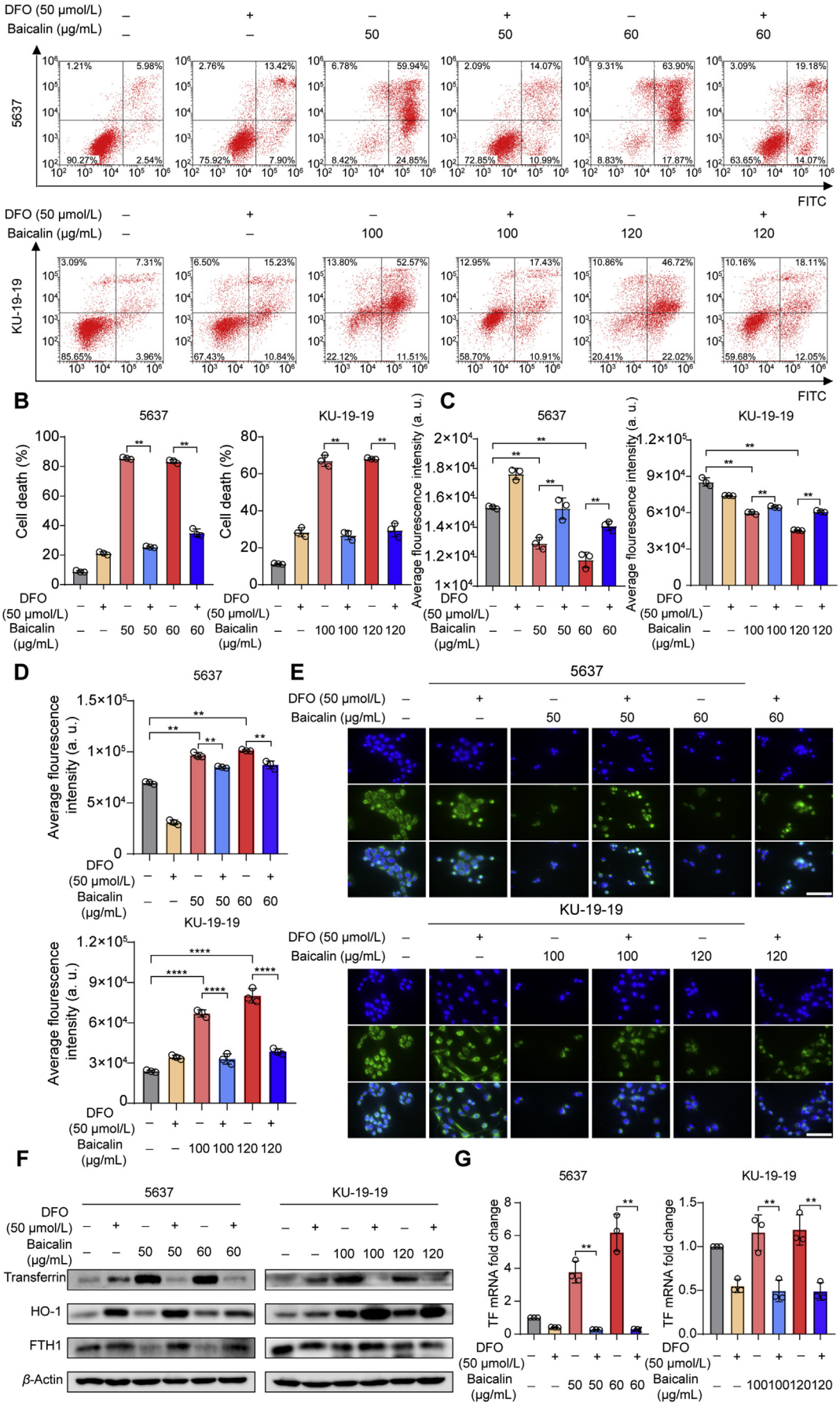
DFO (50 μmol/L)
Baicalin (μg/mL)
5637
KU-19-19
FITC
B
C
D
E
F
G
Cell death (%)
Average flourescence intensity (a. u.)
TF mRNA fold change
Transferrin
HO-1
FTH1
β-Actin

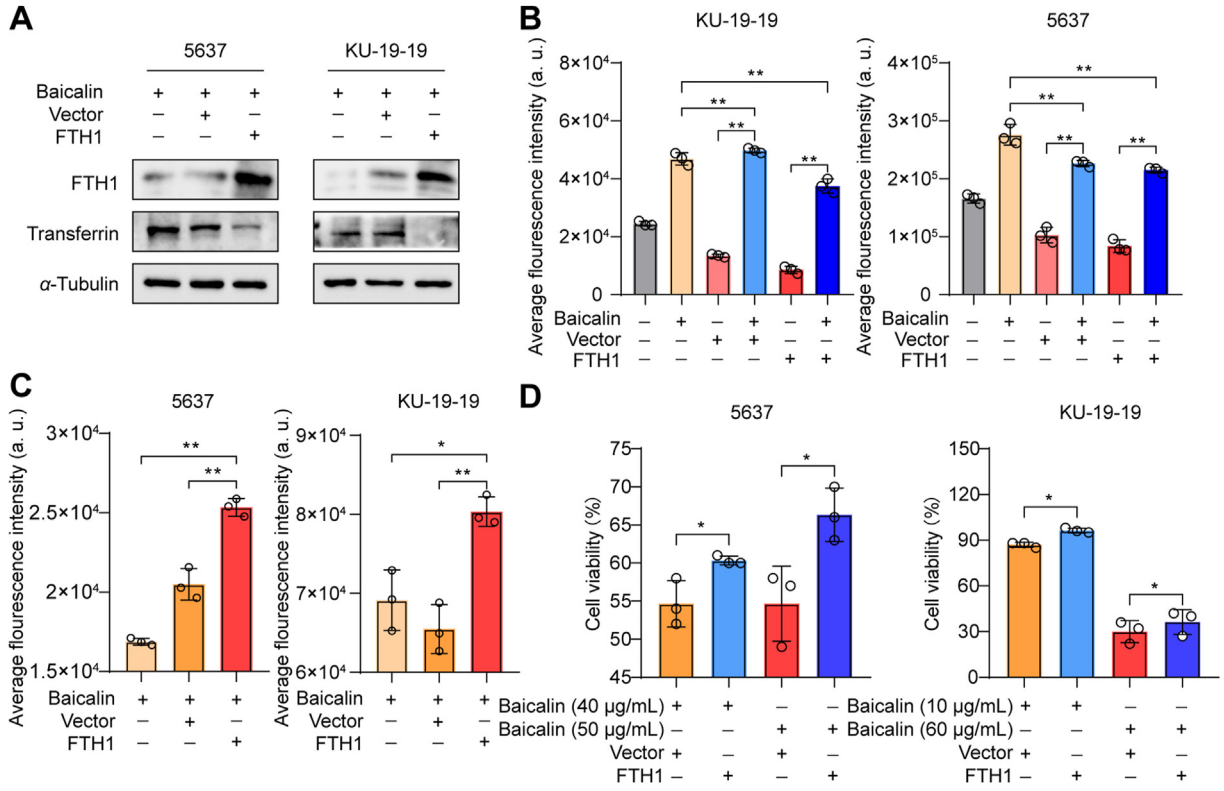

Figure 4 FTH1 was a key determinant for baicalin-induced ferroptosis. (A) The expression of FTH1 and transferrin was detected by Western blotting. (B) Untransfected cells and FTH1-transfected cells were treated with or without baicalin for 24 h and then ROS level was detected, mean ± SD, $n = 3$; $^{**}P < 0.01$. (C) FTH1-transfected 5637 and KU-19-19 cells were treated with baicalin for 24 h and then intracellular chelate iron was analyzed, mean ± SD, $n = 3$; $^{*}P < 0.05$, $^{**}P < 0.01$. (D) FTH1-transfected 5637 and KU-19-19 cells were treated with baicalin for 24 h and then the cell viability was detected by CCK-8, mean ± SD, $n = 3$; $^{*}P < 0.05$.

treatment triggered a decrease in the proportion of Phen Green SK-positive cells, indicating that ferroptosis was triggered (Fig. 3C). Then, ROS were explored by immunofluorescence and DCFH-DA fluorescent probe. As a result, baicalin treatment-induced ROS accumulation in bladder cancer cells (Fig. 3D). Because mitochondria are major sources of ROS within the cell, we next detected the mitochondrial damage by Mito-Tracker Green staining. As shown in Fig. 3E, baicalin treatment triggered mitochondrial damage and cell death. Moreover, these critical events could be rescued by co-treatment with iron chelator DFO (Fig. 3C–E).

In the subsequent experiments, we detected the effect of co-treatment with baicalin and iron chelator DFO on the ferroptotic protein expression. The expression of transferrin (TF), which is responsible for the transport of iron into cells, was increased following treatment with baicalin (Fig. 3F). In contrast, the expression of a negative ferroptosis-regulated protein (FTH1 and HO-1) was decreased (Fig. 3F). Moreover, DFO treatment could abolish the ferroptosis induced by baicalin treatment, which was confirmed by Western blotting. Besides, the transcriptional expression of transferrin was consistent with its protein expression when the bladder cancer cells were treated with baicalin with or without DFO (Fig. 3G). Taken together, these findings strongly suggested that baicalin triggered ferroptotic cell death in bladder cancer cells.

3.3. *FTH1 was a key determinant for baicalin-induced ferroptosis*

To detect whether FTH1 plays an important role in ferroptosis induced by baicalin, 5637 and KU-19-19 cells were transfected with FTH1 plasmid with or without baicalin. The data show FTH1 over-expression significantly decreased the expression of transferrin, indicating baicalin-induced ferroptosis was attenuated (Fig. 4A). We found that as long as baicalin was added, the level of ROS in the cells always increased significantly. In addition, the intracellular ROS level of the bladder cancer cells transfected by FTH1 was remarkably lower than that in untransfected cells (Fig. 4B); however, higher intracellular

Figure 3 DFO could trigger significantly the treatment of baicalin in bladder cancer cells. (A) and (B) The cell death was observed by flow cytometer with the treatment of baicalin with or without DFO, mean ± SD, $n = 3$, $^{**}P < 0.01$. (C) 5637 and KU-19-19 were treated with baicalin along with or without DFO for 24 h, then intracellular chelate iron was analyzed, mean ± SD, $n = 3$; $^{*}P < 0.05$, $^{**}P < 0.01$. (D) The reactive oxygen species (ROS) level was analyzed by a flow cytometer, mean ± SD, $n = 3$; $^{**}P < 0.01$. (E) Mito-Tracker Green staining was made to detect mitochondria damage. Scale: 100 μm. (F) The expression of FTH1, HO-1, transferrin in bladder cancer cells was detected after the treatment with baicalin with or without DFO for 24 h by Western blotting. (G) qRT-PCR was performed to detect the mRNA expression of transferrin, mean ± SD, $n = 3$; $^{**}P < 0.01$.

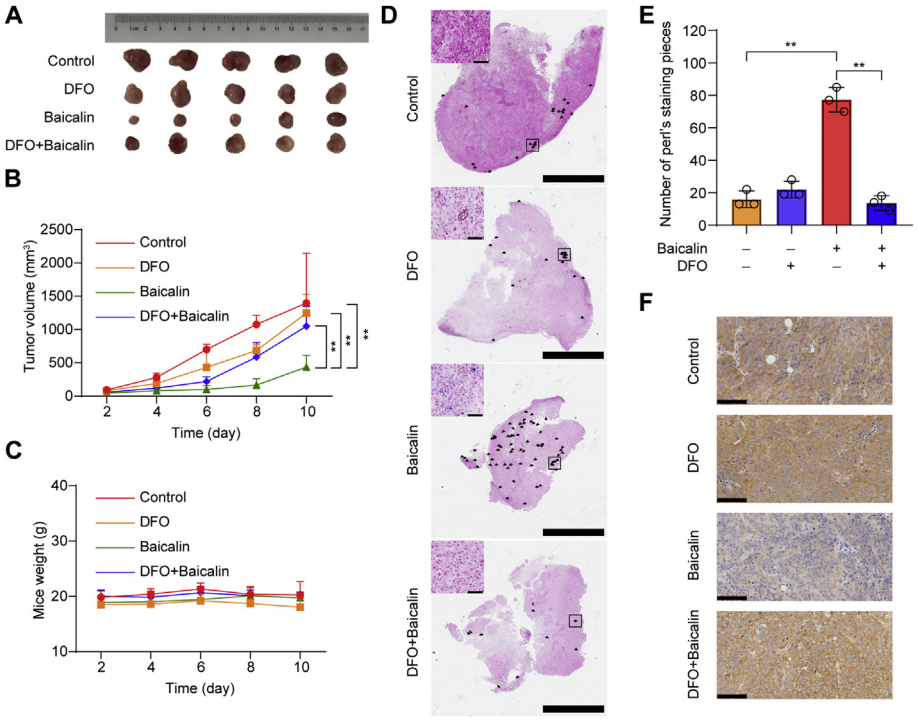

Figure 5 Baicalin triggered ferroptosis in bladder cancer xenograft model. (A) An image of tumor samples in each group. (B) Tumor volume in each group was analyzed. Data are expressed as the mean ± SD, $n = 3$; $^{**}P < 0.01$. (C) Mice weight in each group was analyzed. (D) and (E) Representative results of free iron deposition and quantitative analysis, mean ± SD, $n = 3$; $^{**}P < 0.01$. Scale: 50 μm and 2.5 mm. (F) The expression of FTH1 was determined by immunohistochemical staining. Scale: 120 μm.

chelate iron was observed after FTH1 overexpression (Fig. 4C). Moreover, overexpression of FTH1 significantly abrogated the anticancer effects of baicalin in both 5637 and KU-19-19 cells (Fig. 4D). So, these results suggest that FTH1 was a critical regulator for baicalin-induced ferroptosis in bladder cancer cells.

3.4. Baicalin triggered ferroptosis in bladder cancer xenograft model

To investigate the therapeutic potential effect of baicalin *in vivo*, a subcutaneous xenograft model was performed. When the xenografts reached about 70 mm^3 in size, the mice were randomly divided into four experimental groups (five mice per group): the control group (solvent), baicalin treatment group (200 mg/kg), DFO group (100 mg/kg) and DFO plus baicalin group. As shown in Fig. 5A and B, a significant decrease in tumor volume was detected in the baicalin treatment group compared with those observed in their control group. Moreover, iron chelator DFO treatment could antagonize the anticancer effect of baicalin in bladder cancer cells. However, the mice weights were not affected by baicalin treatment (Fig. 5C), indicating no notable toxicity. Then we investigated the effect of baicalin on ferroptosis by immunohistochemical and Prussian blue staining. Prussian blue staining shows that, compared with the control group, the deposition of free iron in cells was significantly increased in baicalin-treated mice (Fig. 5D and E). Immunohistochemical staining indicated FTH1 expression was decreased in the baicalin treatment group compared with those observed in their control group (Fig. 5F). Taken together, our results demonstrated that baicalin triggered ferroptosis in bladder cancer *in vivo*.

4. Discussion and conclusions

Ferroptosis, a novel cell death form characterized by the iron-dependent accumulation of lipid peroxidation, has recently been recognized as a tumor suppression mechanism in cancer therapy, particularly in the eradication of malignant tumors resistant to conventional therapies[19,20]. Many research also demonstrated that there was a DNA damage-dependent ferroptosis, in which multiple interrelated pathways eventually lead to ferroptosis[21–23]. In recent years, increasing studies have been made in finding novel anticancer drugs based on ferroptosis. Given that natural compounds are the important sources for new anticancer drugs, those natural chemicals that have the potential to induce ferroptosis in cancer are attracting growing interest.

Baicalin, the major bioactive flavones extracted from the roots of *S. baicalensis* Georgi (Scutellariae Radix), also called "Huangqin" in traditional Chinese medicine. Increasing evidence support that baicalin has a potential role in cancer treatment. Baicalin could suppress cell proliferation and migration triggered apoptosis and cell cycle arrest[24–26]. However, the function of baicalin leading to ferroptosis and bladder cancer has been unexplored.

Here, we show that baicalin developed its anticancer activity through inducing apoptosis and cell death in bladder cancer in a dose-dependent manner. Subsequently, we demonstrate for the first time that baicalin triggered ferroptosis *in vitro* and *in vivo*, as evidenced by ROS accumulation and intracellular chelate iron enrichment. Mechanistically, we show FTH1 is a critical mediator for baicalin-induced ferroptosis in bladder cancer cells.

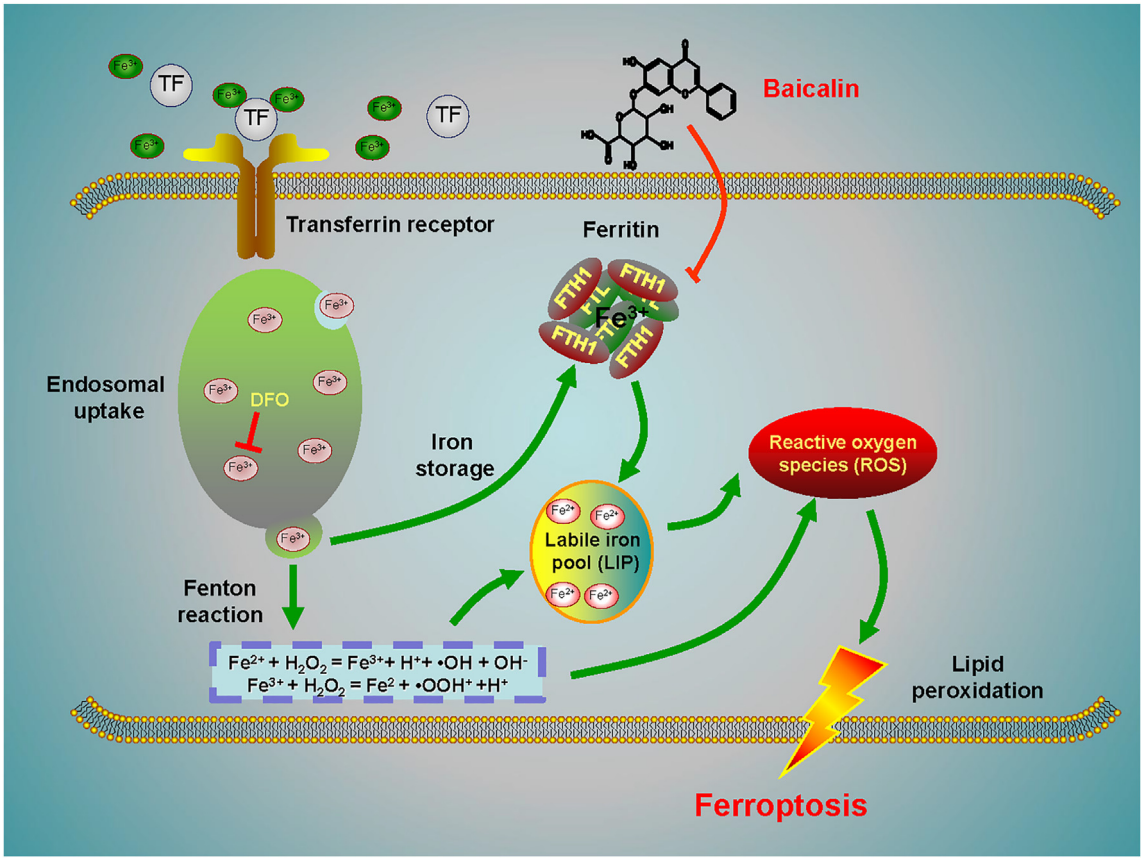

Figure 6 A schematic diagram about the central role of baicalin in ferroptosis induction in bladder cancer. Baicalin exerts its anticancer activity in bladder cancer by inducing FTH1-dependent ferroptosis, which will hopefully provide great therapeutic potential for bladder cancer treatment.

Overexpression of FTH1 abrogated the anticancer effects of baicalin both *in vitro* and *in vivo*. In summary, our investigations demonstrate the natural compound baicalin exerted its anticancer effect by triggering FTH1-dependent ferroptosis, which could provide a ferroptosis inducer for bladder cancer treatment (Fig. 6).

Acknowledgments

This work is supported by the grants National Natural Science Foundation of China (Nos. 81874380 and 82022075, to Xinbing Sui; 81730108 and 81973635, to Tian Xie), Zhejiang Provincial Natural Science Foundation of China for Distinguished Young Scholars (No. LR18H160001, to Xinbing Sui), Zhejiang Provincial Natural Science Foundation of China (Nos. LQ20H160013, Ting Duan; LQ21H160038, to Jiao Feng), and Zhejiang Province Science and Technology Project of TCM (Nos. 2019ZZ016, to Xinbing Sui; 2020ZQ046, to Ruonan Zhang, China).

Author contributions

Xinbing Sui, Tian Xie, and Wei Tao guided and designed the research; Xiaying Chen and Na Kong performed all the experiments. Jiao Feng, Ting Duan, Shuiping Liu, and Xueni Sun provided major technical supports. Peng Chen, Ting Pan, Lili Yan, Ting Jin, Yu Xiang, Quan Gao and Chenyong Wen contributed materials information gathering and data analysis. Weirui Ma, Wencheng Liu, Mingming Zhang, Zuyi Yang, Wengang Wang, Ruonan Zhang and Bi Chen collected and analyzed the data. Xinbing Sui and Xiaying Chen wrote manuscript with contributions from the other authors.

Conflicts of interest

The authors declare no competing interests.

References

1. Yu B, Choi B, Li W, Kim DH. Magnetic field boosted ferroptosis-like cell death and responsive MRI using hybrid vesicles for cancer immunotherapy. *Nat Commun* 2020;**11**:3637.
2. Wang J, Yin X, He W, Xue W, Zhang J, Huang Y. SUV39H1 deficiency suppresses clear cell renal cell carcinoma growth by inducing ferroptosis. *Acta Pharm Sin B* 2021;**11**:406−19.
3. Alu A, Han X, Ma X, Wu M, Wei Y, Wei X. The role of lysosome in regulated necrosis. *Acta Pharm Sin B* 2020;**10**:1880−903.
4. Qiu Y, Cao Y, Cao W, Jia Y, Lu N. The application of ferroptosis in diseases. *Pharmacol Res* 2020;**159**:104919.
5. Stockwell BR, Jiang X, Gu W. Emerging mechanisms and disease relevance of ferroptosis. *Trends Cell Biol* 2020;**30**:478−90.
6. Badgley MA, Kremer DM, Maurer HC, DelGiorno KE, Lee HJ, Purohit V, et al. Cysteine depletion induces pancreatic tumor ferroptosis in mice. *Science* 2020;**368**:85−9.
7. Lee H, Zandkarimi F, Zhang Y, Meena JK, Kim J, Zhuang L, et al. Energy-stress-mediated AMPK activation inhibits ferroptosis. *Nat Cell Biol* 2020;**22**:225−34.

8. Zhou QM, Wang S, Zhang H, Lu YY, Wang XF, Motoo Y, et al. The combination of baicalin and baicalein enhances apoptosis *via* the ERK/p38 MAPK pathway in human breast cancer cells. *Acta Pharmacol Sin* 2009;**30**:1648−58.
9. Tan HY, Wang N, Man K, Tsao SW, Che CM, Feng Y. Autophagy-induced RelB/p52 activation mediates tumour-associated macrophage repolarisation and suppression of hepatocellular carcinoma by natural compound baicalin. *Cell Death Dis* 2015;**6**:e1942.
10. Wei Y, Liang J, Zheng X, Pi C, Liu H, Yang H, et al. Lung-targeting drug delivery system of baicalin-loaded nanoliposomes: development, biodistribution in rabbits, and pharmacodynamics in nude mice bearing orthotopic human lung cancer. *Int J Nanomed* 2017;**12**: 251−61.
11. Lin C, Tsai SC, Tseng MT, Peng SF, Kuo SC, Lin MW, et al. AKT serine/threonine protein kinase modulates baicalin-triggered autophagy in human bladder cancer T24 cells. *Int J Oncol* 2013;**42**: 993−1000.
12. Peng H, Xu Z, Wang Y, Feng N, Yang W, Tang J. Biomimetic mesoporous silica nanoparticles for enhanced blood circulation and cancer therapy. *ACS Appl Bio Mater* 2020;**3**:7849−57.
13. Gilbert LA, Larson MH, Morsut L, Liu Z, Brar GA, Torres SE, et al. CRISPR-mediated modular RNA-guided regulation of transcription in eukaryotes. *Cell* 2013;**154**:442−51.
14. Bock FJ, Tait SWG. Mitochondria as multifaceted regulators of cell death. *Nat Rev Mol Cell Biol* 2020;**21**:85−100.
15. Westermann B. Mitochondrial fusion and fission in cell life and death. *Nat Rev Mol Cell Biol* 2010;**11**:872−84.
16. Dawson TM, Dawson VL. Mitochondrial mechanisms of neuronal cell death: potential therapeutics. *Annu Rev Pharmacol Toxicol* 2017;**57**: 437−54.
17. Guo S, Yao X, Jiang Q, Wang K, Zhang Y, Peng H, et al. Dihydroartemisinin-loaded magnetic nanoparticles for enhanced chemodynamic therapy. *Front Pharmacol* 2020;**11**:226.
18. Yang X, Yu D, Xue L, Li H, Du J. Probiotics modulate the microbiota−gut−brain axis and improve memory deficits in aged SAMP8 mice. *Acta Pharm Sin B* 2020;**10**:475−87.
19. Bersuker K, Hendricks JM, Li Z, Magtanong L, Ford B, Tang PH, et al. The CoQ oxidoreductase FSP1 acts parallel to GPX4 to inhibit ferroptosis. *Nature* 2019;**575**:688−92.
20. Liang C, Zhang X, Yang M, Dong X. Recent progress in ferroptosis inducers for cancer therapy. *Adv Mater* 2019;**31**:e1904197.
21. Li C, Zhang Y, Liu J, Kang R, Klionsky DJ, Tang D. Mitochondrial DNA stress triggers autophagy-dependent ferroptotic death. *Autophagy* 2020;**17**:948−60.
22. Song X, Xie Y, Kang R, Hou W, Sun X, Epperly MW, et al. FANCD2 protects against bone marrow injury from ferroptosis. *Biochem Biophys Res Commun* 2016;**480**:443−9.
23. Chen PH, Wu J, Ding CC, Lin CC, Pan S, Bossa N, et al. Kinome screen of ferroptosis reveals a novel role of ATM in regulating iron metabolism. *Cell Death Differ* 2020;**27**:1008−22.
24. Wang Z, Ma L, Su M, Zhou Y, Mao K, Li C, et al. Baicalin induces cellular senescence in human colon cancer cells *via* upregulation of DEPP and the activation of Ras/Raf/MEK/ERK signaling. *Cell Death Dis* 2018;**9**:217.
25. Chen H, Gao Y, Wu J, Chen Y, Chen B, Hu J, et al. Exploring therapeutic potentials of baicalin and its aglycone baicalein for hematological malignancies. *Cancer Lett* 2014;**354**:5−11.
26. Yang B, Bai H, Sa Y, Zhu P, Liu P. Inhibiting EMT, stemness and cell cycle involved in baicalin-induced growth inhibition and apoptosis in colorectal cancer cells. *J Cancer* 2020;**11**:2303−17.